Article

JOURNAL OF COMPOSITE MATERIALS

Journal of Composite Materials
46(7) 755–763

DOI: 10.1177/0021998311410503
jcm.sagepub.com

SAGE

# Zn–Al-based metal–matrix composites with high stiffness and high viscoelastic damping

**T Jaglinski and RS Lakes**

**Abstract**

A maximal product of stiffness and viscoelastic damping ($E$ tan $\delta$), a figure of merit for damping layers, is desirable for structural damping applications. Particulate-reinforced metal–matrix composites were prepared by ultrasonic agitation of the melt and composed of the zinc–aluminum (ZnAl) alloy $Zn_{80}Al_{20}$ (in wt%) as the lossy matrix and SiC or $BaTiO_3$ as the particulate reinforcements. ZnAl–SiC composites were stiffer and exhibited higher damping at acoustic frequencies in comparison to the base alloy. ZnAl–SiC composites were superior to Sn–SiC composites and possessed an $E$ tan $\delta$ in excess of 0.6 GPa, the maximum figure of merit provided by commercial polymer damping layers. Furthermore, ZnAl–SiC composites displayed a high figure of merit over a broad temperature range. ZnAl–$BaTiO_3$ composites exhibited anomalies in modulus and damping associated with partial restraint of the phase transformation; one specimen was much stiffer than diamond over a narrow temperature range.

**Keywords**

Metal–matrix composites, viscoelasticity, dynamic properties, vibration damping

## Introduction

A maximal combination of stiffness and viscoelastic damping (typically the product $|E^*|\tan\delta$) is desirable for damping layer and structural damping applications where reduction of vibration in machinery and vehicles is desirable. $|E^*|$ is the absolute value of the complex, dynamic Young's modulus ($E' + iE''$), and $\delta$ the phase angle between stress and strain. For low-damping materials, measures of modulus coincide; the absolute value $|E^*|$ is referred to as $E$ hereafter. The figures of merit for stiff structural metals such as brass, steel, and aluminum alloys are low because viscoelastic effects are usually small; tan $\delta$ is typically $10^{-6}$ to $10^{-3}$. Polymer damping layers provide $E \tan\delta < 0.6$ GPa, shown as the diagonal lines in Figure 1 (left and right), because of their higher damping, tan $\delta$ of 0.1–1, but despite their relatively low stiffness, as is the case with most high damping materials (Figure 1, left).[1] The temperature dependence and frequency dependence of polymeric damping layers can be problematic. An example of these properties is shown as a function of temperature for a polymer blend over an extended temperature range in Figure 1 (right). Specifically, for high-damping polymer layers,[2] the full width at half maximum of the damping peak at constant frequency may be only about 18°C. So, a temperature change of 9°C off peak reduces the effective damping by a factor of two, mitigating the effectiveness of the layer. Some polymer layers are designed for a broader temperature range but the performance suffers.

Metal–matrix composites (MMCs) which possess both high damping and high stiffness are of interest in achieving better performance for structural damping applications. Analysis shows Reuss laminates and particulate morphologies (where the particulates are the stiff phase) can be used to achieve maximal $E$ tan $\delta$. Particulate inclusions are superior to fibers in composites intended for damping, even though particles contribute less to the effective composite stiffness for a given volume fraction. For both laminates and

Department of Engineering Physics, Engineering Mechanics Program University of Wisconsin, Madison, USA

**Corresponding author:**
T. Jaglinski, Department of Engineering Physics, Engineering Mechanics Program University of Wisconsin, Madison, WI 53706-1687, USA
Email: tmjaglinski@gmail.com

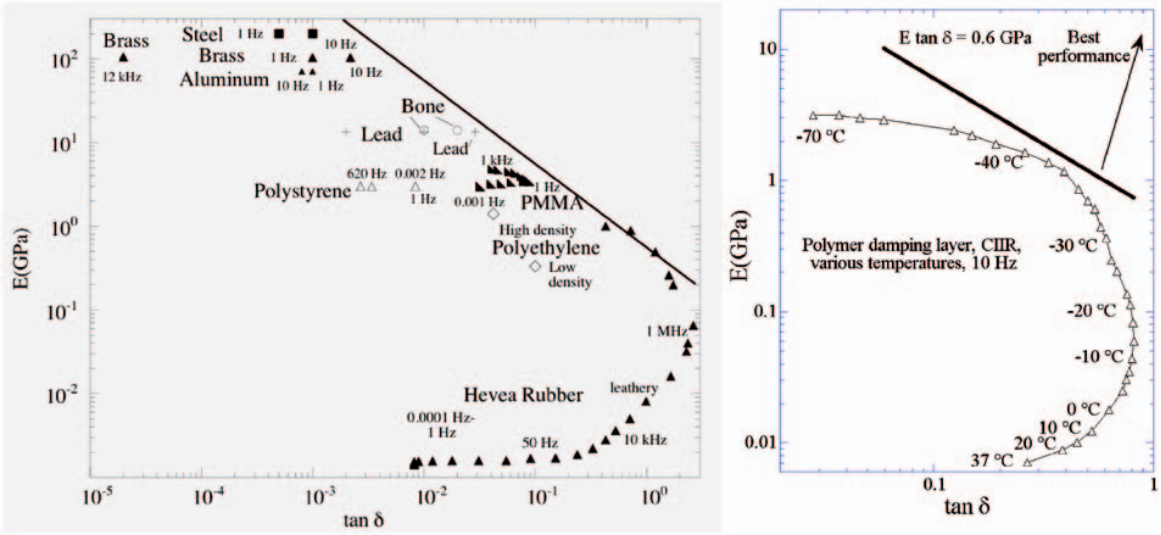


**Figure 1.** Stiffness–loss map showing (left) common materials and[1] (right) polymer damping layer (type CIIR) intended for a comparatively wide range of temperature at a constant frequency of 10 Hz.[2]

particulate composites, the stiff phase is as stiff as possible and the high damping phase has the maximum tan δ possible. Several composites developed as proof of concept include laminar W–InSn[3] and particulate SiC–InSn.[4,5] Such composites cannot support much stress because the weak matrix is fully stressed. Low matrix strength is not a problem if the material is to be used as a damping layer, but strength is needed as well as high $E$ tan δ for materials used in structures.

Zinc–aluminum alloys (ZnAl) as a matrix material are of interest for the following reasons. ZnAl alloys are already widely used as industrial casting alloys and are sufficiently stiff and strong for many applications. They have been well studied in the context of their damping[6] and phase transformations.[7] ZnAl alloys have melting temperatures in the order of 450°C (compared with Sn at 230°C) allowing moderate processing temperatures and reasonably high service temperatures. The density of the alloys can be titrated to match the density of the inclusions to minimize segregation from buoyancy in the melt before solidification ($\rho_{Zn} = 7.14$ g/cc and $\rho_{Al} = 2.7$ g/cc). The stiffness of ZnAl (depending on composition) is about a factor of 1.5 to 2 greater than that of Sn; the intrinsic damping is similar and the strength is much greater. As for particulate inclusions as passive stiffening agents, silicon carbide (SiC) particles are attractive since SiC has high stiffness, $E = 430$ GPa, low density, $\rho = 3.2$ g/cm$^3$, and reasonable cost.[8]

Composites utilizing phase-transforming inclusions are based on the concept of negative stiffness. In the Landau theory of phase transformations, the strain energy function contains a single minimum which flattens during cooling, indicating softening of the modulus; two minima are then formed indicating instability. The curvature of the energy function between minima indicates a negative modulus. This is not observed in a free block of material but can be stabilized by the matrix of a composite. Extremely high values of stiffness (even greater than that of diamond) and damping have been achieved in Sn–$BaTiO_3$[9] by use of the incipient phase transformations of the ceramic inclusions. Analysis based on Hashin–Shtrikman (HS) bounds contains a tacit assumption that both constituents are in a minimum energy state; therefore, such analysis does not apply to composites with constrained transforming inclusions. Here too, a stronger matrix is of interest because in these composites, local strain near the inclusions greatly exceeds macroscopic strain.

The purposes of this study are to develop fabrication methods for high damping particulate MMCs, to explore ZnAl alloys as matrix material, and to characterize the viscoelastic response of the composites with the overall aim of achieving composites with maximal $E$ tan δ.

## Materials and methods

### *Materials and processing*

Matrix alloy compositions studied were $Zn_{90}Al_{10}$, $Zn_{80}Al_{20}$, and $Zn_{70}Al_{30}$ in wt%. These alloys, which have moduli near to that of pure Zn, were chosen as the lossy matrix for the composites for reasons given in the introduction. Composites utilizing passive and dynamic inclusion reinforcements were prepared; for

all composites, $Zn_{80}Al_{20}$ was used as the matrix material. For passive inclusions, silicon carbide (SiC) was chosen as the stiff reinforcement; barium titanate ($BaTiO_3$) was used as dynamic inclusions, similar to Sn–$BaTiO_3$ composites tested previously.[9] SiC particles of approximately 125 μm (120 grit) and 20 μm (1000 grit) were obtained from Buehler and were used as-received. Large $BaTiO_3$ pieces were obtained from Alfa Aesar, hand ground with a mortar and pestle, and sieved to achieve a particle size range of 150 and 210 μm. For comparison with the ZnAl–SiC composites, Sn–SiC composites were prepared.

Constituents for the ZnAl alloys were melted in an alumina crucible and poured into a 6061 aluminum alloy mold. Castings were easily removable with no adhesion to the mold. In this study, 10 mm Zn and 15 mm Al shots (Alfa Aesar, both 99.99% metals basis) were used for all castings. Composites were prepared by ultrasonic casting using a Misonix S-4000 sonicator with a 1/2″ diameter standard horn and 1/2″ diameter titanium extension rod. Melts were agitated directly by placing the extension rod about 1.5 times the rod diameter into the melts; sonication time was about 10 min in all cases. The amplitude of the sonication was set to a level of 80 of a maximum of 100 arbitrary units. Particles were added in small increments. Some scraping of the side of crucible with an alumina rod was required to free trapped particles. Once all particles were incorporated (usually in about 7 min), the melt was allowed to sonicate for the remaining 10 min. A similar method has been used previously[10] to create low-concentration dispersions of nano-sized particles with the aim of enhancing strength. Samples for dynamic mechanical testing were sectioned using a low-speed, abrasive diamond saw. Wire electric discharge machining was used to prepare flat, dog bone-shaped specimens for tensile testing having dimensions $35 \times 5 \times 2\,mm^3$ in the gage section. Flat sides were polished to a 800 grit finish.

## *Characterization*

Elastic properties of the matrix alloys were determined using wave transmission ultrasound. Ultrasonic longitudinal waves at 10 MHz and shear waves at 5 MHz were generated *via* a pulse generator/receiver (Panametrics Model 500 PR) and standard piezoelectric transducers. The longitudinal wave speed revealed the tensorial modulus $C_{11}$, and the shear wave speed the shear modulus. Young's modulus and Poisson's ratio were calculated assuming the alloys and composites to be isotropic. Based upon the observed random microstructures of the cast alloys and of the particulate composites (see Figure 6, for example), an isotropic assumption is justified.

Determination of strength was done at a constant deformation rate of $1.33 \times 10^{-4}$ in./s ($33.8 \times 10^{-4}$ mm/s, for a strain rate of ~$1 \times 10^{-4}$/s) and ambient temperature using a screw-driven MTS Sintech 10GL test frame with a 10,000-lb load cell and accompanying Testworks software.

Viscoelastic properties of matrix alloys and composites were evaluated at ambient temperature (23–25°C) using a modified[11] broadband viscoelastic spectroscopy (BVS) apparatus.[12] This device, shown in Figure 2, was used to measure the loss angle δ and the dynamic Young's and shear moduli at audio and sub-audio frequencies. The fixed end of each specimen was mechanically clamped between two tungsten flat-to-round adapters and then onto a 1-in. diameter steel support rod. Sample sizes were about $1 \times 2 \times 20\,mm^3$; bending occurred about the thin dimension. Natural frequencies were typically about 600 Hz in bending and 7 kHz in torsion. Magnets were glued to the free end with cyanoacrylate cement for room temperature tests and Micro Measurements Mbond 610 strain gage cement for elevated temperature tests. Sinusoidal torque was produced electromagnetically by a Helmholtz coil acting upon the high-intensity Nd–Fe–B magnet (for room temperature) or Sm–Co-based magnet (for elevated temperature). Angular displacement was measured *via* laser light reflected from a small mirror at the free end of the sample to a semiconductor light detector. The laser beam was verified to be within the detector area during testing. This technique is capable of measuring tan δ at subresonant frequencies from $10^{-3}$ Hz to more than 1 kHz and for resonant frequencies including overtones up to about $10^5$ Hz. If creep is also done, a range of 11 decades (a factor of $10^{11}$ in time and frequency) can be studied. By contrast, commercial dynamic mechanical analyzers cover only a few decades below the audio range. Phase angle was determined using a lock-in amplifier (Stanford Research SRS 850). The lower limit on frequency is dictated by the experimenters' patience. Time–temperature shifts are not used; all properties are measured directly. The method is particularly advantageous for composites which, unlike amorphous polymers, do not obey time temperature superposition. This study is concerned with vibration damping and sound absorption, so neither very low-frequency testing nor creep was done. Surface strain amplitude of the subresonant oscillations was in the order of $10^{-6}$, well within the linear range of behavior.

Viscoelastic properties were also determined at ultrasonic frequency using resonant ultrasound spectroscopy (RUS; Figure 2). In this method, a cube, prism, or short cylinder is gently held by the specimen corners (nearly approximating a freely oscillating body) between two ultrasonic transducers, one of which is excited with a variable frequency signal generator.

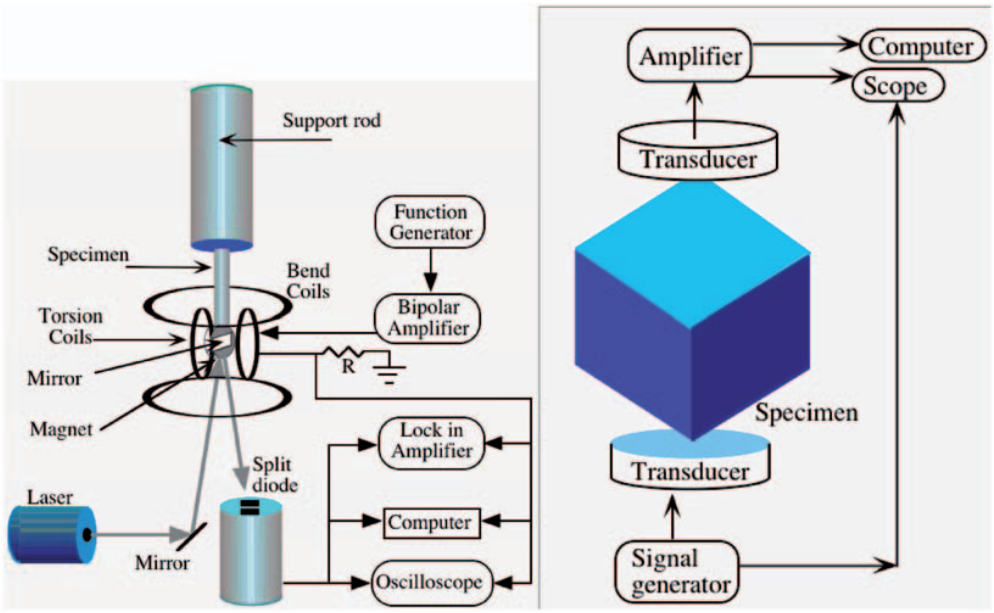


**Figure 2.** Test instruments: (*left*) BVS and (*right*) RUS.

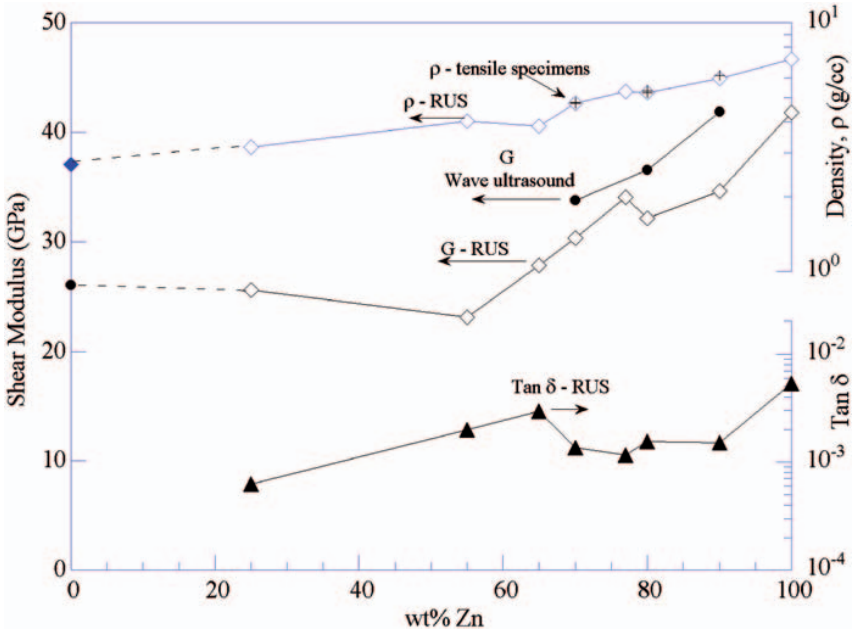


**Figure 3.** Densities, shear moduli, and damping of various ZnAl alloys derived from the fundamental torsional mode determined from RUS measurements on cubic specimens in the frequency range 100–200 kHz (depending on specimen size). *G* for the tensile specimens was obtained *via* wave ultrasound at 5 MHz.

Response of the receiving transducer is captured *versus* frequency. For this study, cubes were used with side lengths between 3 and 5 mm. The mode structure for isotropic cubes[13] as a function of Poisson's ratio has been computed numerically, allowing the fundamental mode to be clearly identified *via* comparison of measured and numerical frequency ratios for the lowest few modes. The shear modulus was calculated from the fundamental natural frequency, the density, and the dimensions of the specimen. At the fundamental resonance, the damping was determined from resonant half width measurement.

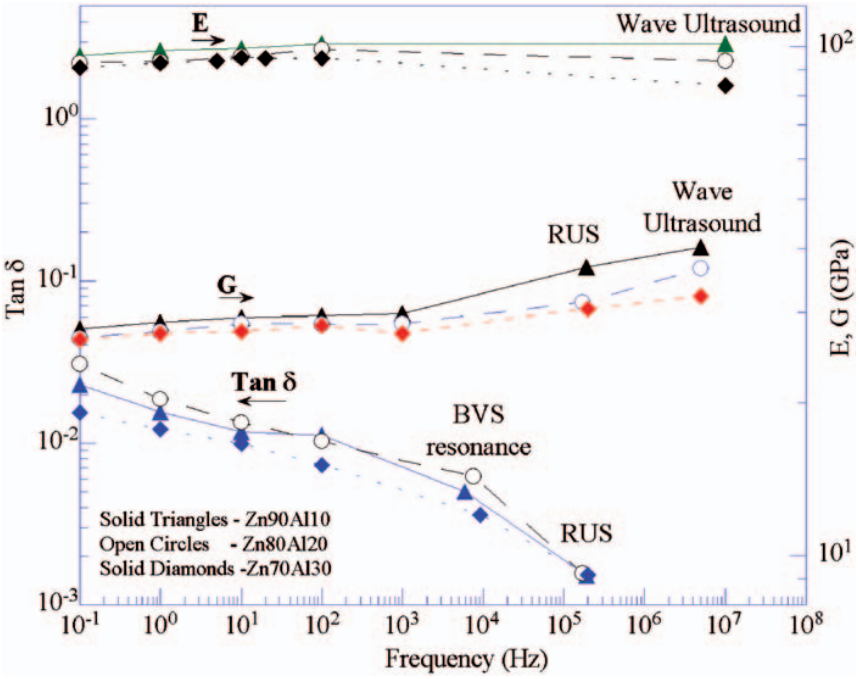


**Figure 4.** *E*, *G*, and tan δ of present ZnAl matrix alloys as a function of frequency. Tan δ in bending is similar to that of torsion and is not shown for clarity.

## Results and discussion

The ultrasonic casting approach yielded good dispersions and satisfactory composites for the 125 μm particle size for both inclusion types and for both the ZnAl and Sn matrices. By contrast, prior attempts to make similar composites by stir casting did not succeed due to poor wetting. For this study, for a particle size of 125 μm, the upper limit for particle volume fraction was about 40% for both the Sn and ZnAl matrices. With further increases in particle concentration, the melts became highly viscous inhibiting sonication and decreasing fluidity to the point where the mold cavity did not fill properly. Smaller particles of size 20 μm SiC did not incorporate well into the ZnAl melt during sonication; sectioned ingots showed large inclusions of conglomerated particles; further, significant residual powder was found in the crucible slag. Therefore, results are reported for particles of size 125 μm, at concentrations not exceeding 40%.

Figures 3 and 4 show the baseline viscoelastic properties for the ZnAl matrix alloys. As might be expected, density, modulus, and damping increase with zinc concentration. For ultrasonic frequencies of 100–200 kHz, damping is the lowest in the aluminum-rich region and attains a relative maximum at intermediate concentrations. In Figure 3, the shear modulus, *G* for the tensile specimens was obtained *via* wave ultrasound at 5 MHz. Higher moduli at the higher frequencies result from

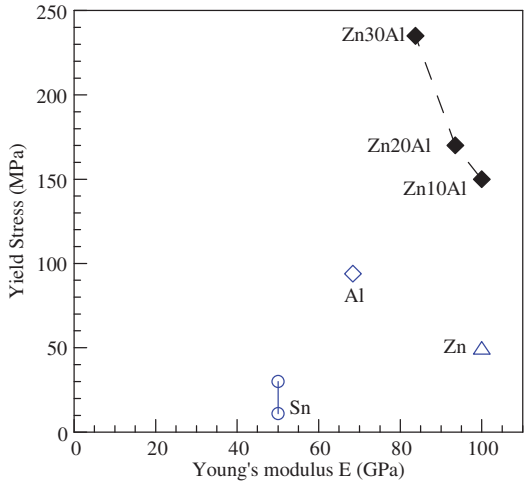


**Figure 5.** Yield stress *vs.* Young's modulus for ZnAl matrix alloys studied as matrix materials. Shown for comparison are properties of pure zinc, aluminum, and tin. Two data points are shown for tin, the lower for pure tin and the upper for commercially pure tin.

viscoelastic dispersion. In the low audio frequency range, these alloys provide high damping (for metals) in the vicinity of 0.01. The combination of modulus, about 95–100 GPa for the present ZnAl alloys, and relatively high damping is favorable for sound and

vibration damping applications (Figure 4). An additional benefit of ZnAl as a matrix material is its considerably greater strength (Figure 5) over that of the pure metals; this includes the tin used in prior composites made to study the effects of inclusion phase transformations. At higher frequencies, the ZnAl alloy damping rolls off. Similarly,[6] damping of Zn27%Al at constant temperature decreased as a power law in frequency. In pure zinc, damping is less dependent on frequency.[14]

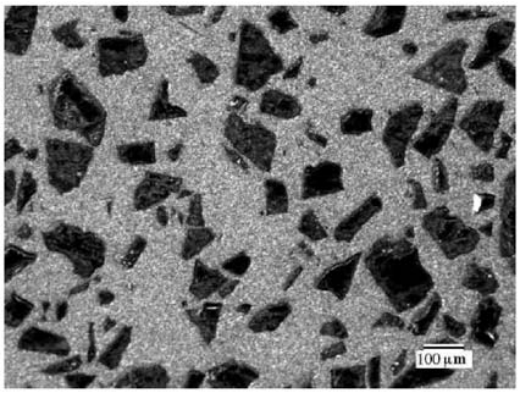


**Figure 6.** Dark field image of the typical microstructure of a 40 vol.% SiC–ZnAl composite. Scale bar is 100 μm.

Figure 6 shows a typical composite microstructure for a 40 vol.% SiC–ZnAl composite with a 125 μm particle size. Figure 7 shows the viscoelastic response of the composites over a range of frequency. Composites were stiffer than the alloy matrix and exhibited higher damping at acoustic frequencies. From composite theory solutions for particulate morphologies,[15] enhanced composite stiffness over the matrix is expected as imparted by the stiffer inclusions. For damping, application of the elastic–viscoelastic correspondence principle to composite theory solutions indicates that composite damping should be lower than that of the matrix for all frequencies. For example, the HS[15] lower bound formula can be used to approximate the behavior of particulate composites provided the

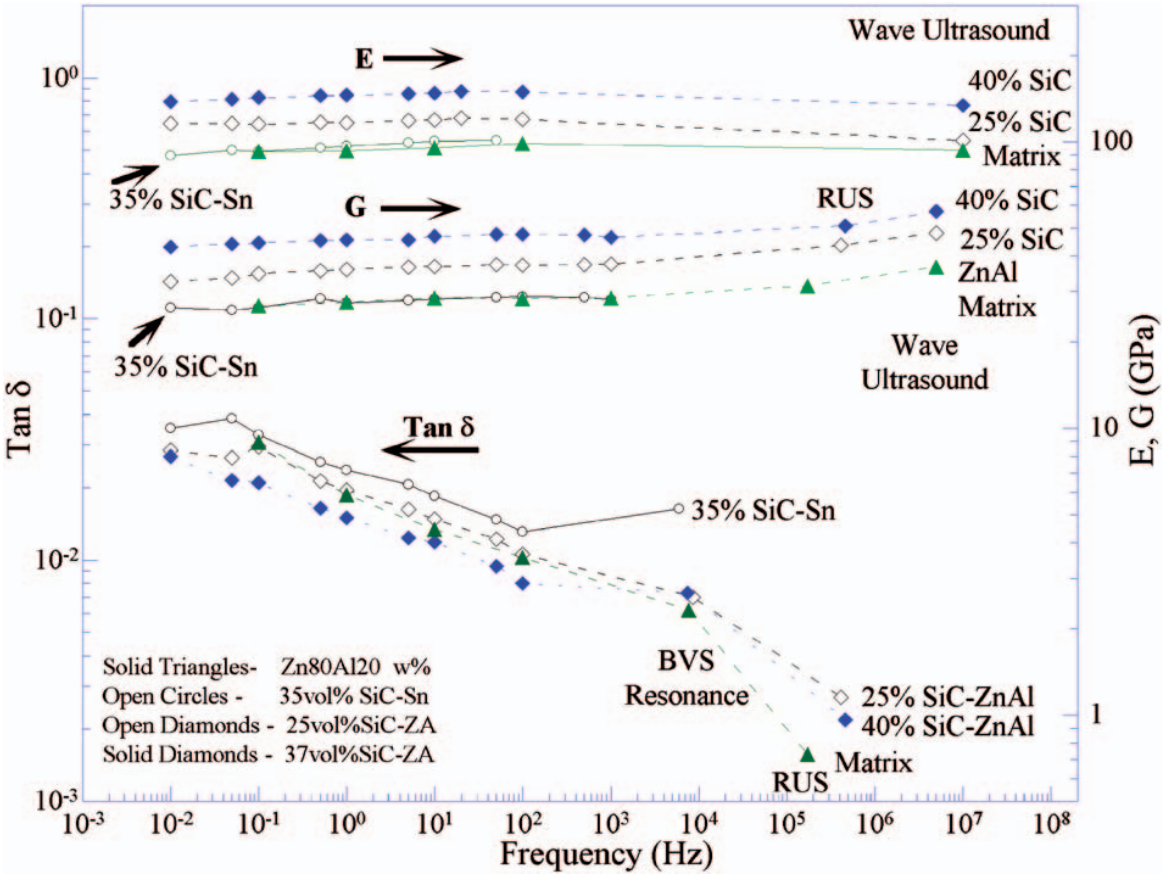


**Figure 7.** *E*, *G*, tan δ from the Zn80Al20 matrix alloy (solid triangles), 25 vol.% SiC–ZnAl (open diamonds), and 40 vol.% SiC–ZnAl (solid diamonds) as well as the 35 vol.% SiC–Sn (open circles) as they depend upon frequency. Damping in torsion is shown; damping in bending (not shown) is similar. All composites use 125-μm sized SiC particles. The matrix material for ZnAl–SiC composites is Zn80Al20 (wt%).

concentration of inclusions is not too high. Though the HS bounds can be realized by coated spherical particulates, irregularity of particle shape has minimal influence on properties below about 40% concentration by volume.[16] Assuming complex moduli in the present analysis to reflect the observed viscoelasticity, evaluation of the HS lower bound predicts the following for composite stiffness and damping. For 25% SiC–ZnAl at 10 Hz, the theoretical stiffening is a factor 1.4, experimentally a factor 1.37; theoretically, tan δ is a reduced factor 0.85. For 40% SiC–ZnAl at 10 Hz, the theoretical stiffening is a factor 1.87, experimentally a factor 1.78; theoretically, tan δ is reduced a factor 0.75. The experimental composite stiffness is in good agreement with the theoretical prediction. However, in regards to damping which is predicted to be reduced at all frequencies, the 25% SiC–ZnAl composite has higher damping than the matrix at all frequencies; substantially higher at ultrasonic frequency. The 40% SiC–ZnAl composite has modestly lower (10–20%) damping than the matrix at low frequencies but substantially higher at ultrasonic frequency. Enhanced damping is indicative of an interaction effect between particle and matrix not captured by composite theory. The effect is attributed to the generation of dislocations in the matrix by stress due to thermal expansion mismatch between matrix and inclusion during cooling from the melt. The effect is beneficial for materials intended for damping applications.

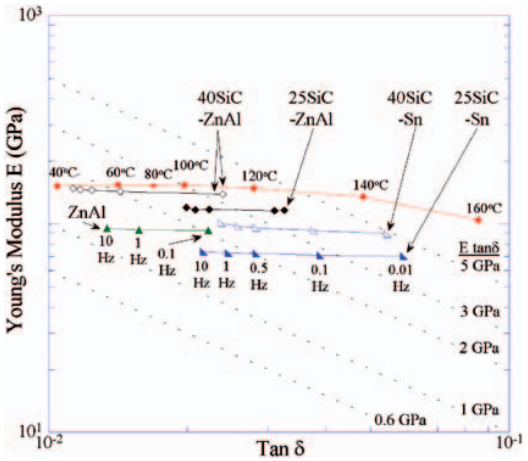


**Figure 8.** Stiffness–loss map, or *E vs.* tan δ, for the present composites and base ZnAl matrix alloys. Isothermal plots for ambient temperature show the frequency range of 10 Hz (on left of curve) to 0.01 Hz (to the right). A constant frequency plot for 40% SiC–ZnAl at 10 Hz at various temperatures is also shown. Plots of the figure of merit for damping layers, *E* tan δ = constant, are shown as diagonal dashed lines for comparison. Polymeric damping layers have a maximum figure of merit in the vicinity of 0.6 GPa. Temperature dependence of such a layer is shown in Figure 1 (right).

Figure 8 is a stiffness–loss map, or *E versus* tan δ, of SiC–ZnAl composites and matrix $Zn_{80}Al_{20}$ alloy. Contours are shown over the frequency range 0.01–10 Hz at ambient temperature as well as a temperature-dependent plot for 40% SiC–ZnAl at 10 Hz.

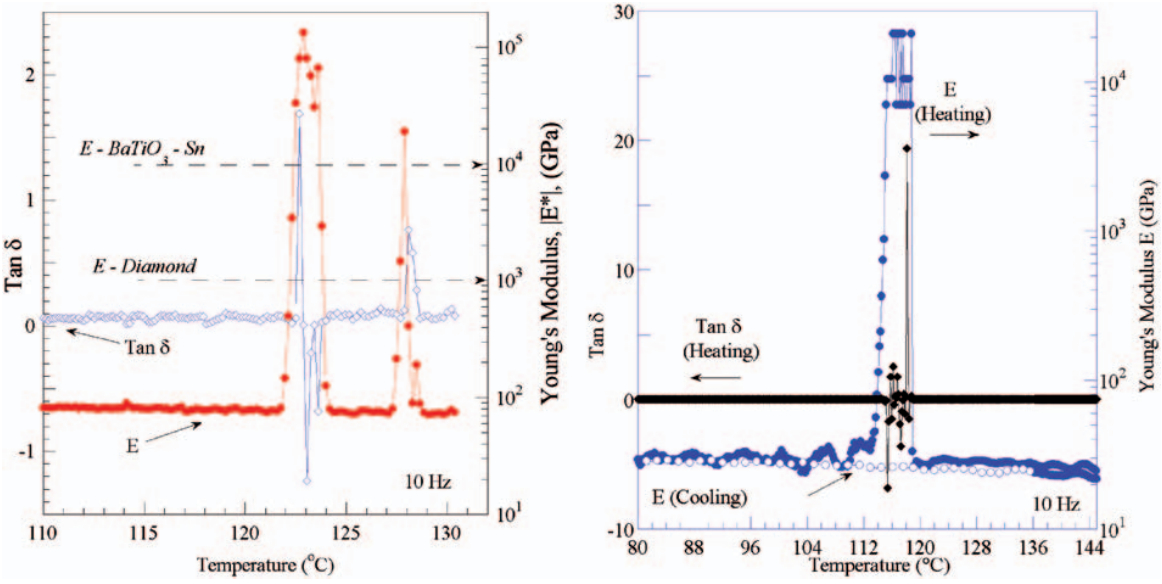


**Figure 9.** (*left*) Large peaks in effective stiffness associated with phase transformations of the $BaTiO_3$ inclusions partially restrained by the ZnAl matrix. (*right*) Similar high temperature peaks in Sn–$BaTiO_3$ composites. Both experiments were conducted at a constant drive frequency of 10 Hz.

Also shown in Figure 8 are contours of $E$ tan δ = constant for comparison. It is noteworthy that the present results are within the linear range of behavior; by contrast high damping in copper–manganese alloys and their composites is nonlinear and requires relatively large strain to activate. The figure of merit for the present composites is superior to that of commercial polymer damping layers (maximum $E$ tan δ of 0.6 GPa). The figure of merit is also greater than that of polymer–nanoclay composites,[17] $E$ tan $\delta \leq 0.3$ GPa. In a related vein, nanotube–polycarbonate and nanotube–epoxy composites exhibit improvement in comparison with the neat resin[18,19] but are still inferior to commercial polymer damping layer materials and much inferior to the SiC–ZnAl composites investigated here. Finally, the temperature dependence of composite damping shown in Figure 8 reveals a wide range of temperature at which the figure of merit is high. This is to be compared with polymer damping layers for which a range of 18°C is representative and 50°C is maximal in polymer blends of reduced performance (Figure 1, right).

Results for 5 vol%$BaTiO_3$–ZnAl composites as a function of temperature at constant frequency (10 Hz) are shown in Figures 9 and 10. As discussed in the 'Introduction' section, these materials contain stored energy so they are not required to obey the classical bounds. Of the seven composites tested, one specimen displayed extreme effective peaks in stiffness (Young's modulus about a hundred times greater than that of diamond) and doublets in damping, as shown in Figure 9 (left). This behavior was observed only on the initial heating scan and was not recovered upon subsequent thermal cycles. Similar behavior was also observed in Sn–$BaTiO_3$ composites, as shown in Figure 9 (right). Enhanced effective stiffness is attributed to the magnification of local strain known to occur in such composites. Two 5%$BaTiO_3$–ZnAl specimens displayed small undulations in stiffness and no change in damping, primarily above the Curie point (near 125°C) of the inclusions (Figure 10). These undulations in stiffness emerged from the initial behavior after several thermal cycles and did not attenuate in amplitude thereafter for up to 12 cycles. One specimen displayed characteristics of material instability, namely phase jitter and transient negative tan δ;[20] the last three samples displayed only monotonic changes in damping and stiffness. These behaviors are not observed in the Sn–SiC and ZnAl–SiC composites. With the present ZnAl matrix material, the smaller anomalies are retained over more thermal cycles than with the Sn matrix;[9] with the Sn matrix, it was necessary to precoat the inclusions but inclusions in the ZnAl matrix were not precoated. Even so, a larger proportion of ZnAl–$BaTiO_3$ composite specimens exhibited anomalies in comparison with Sn–$BaTiO_3$ composites.

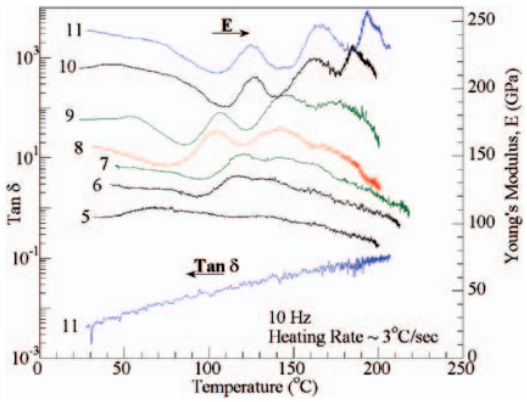


**Figure 10.** Undulations in stiffness upon heating from ambient associated with partially restrained phase transformations in the ZnAl–$BaTiO_3$ composites. Thermal cycles 5–11 are shown as behavior emerged after four thermal cycles and maintained for at least 11 thermal cycles. Curves for stiffness are shifted vertically for clarity from the baseline curve for cycle 5. Only tan δ for cycle 11 is shown, the others are coincident. All experiments were conducted at a constant drive frequency of 10 Hz.

The ZnAl–$BaTiO_3$ composites are capable of extremely high transient values of modulus and damping but they are not yet sufficiently robust to thermal cycling for practical use. It may be necessary to precoat the inclusions to achieve better interface strength. The temperature width of the peak, about 4°C is narrower than that (18°C) of high-loss polymer layers but may be broadened by designed heterogeneity. The center temperature of the anomaly is associated with the Curie point near 125°C, peaks above this could correspond to secondary soft modes, such as[21] in the cubic phase of $BaTiO_3$ near 170°C. Similar high stiffness anomalies have been observed in our laboratory[9,22] in Sn–$BaTiO_3$ composites, as shown in Figure 9 (right). In a related vein, an oxygen vacancy-based transition[23] in the tetragonal phase is likely responsible for the anomalies seen near 70°C (below the Curie point) in Sn–$BaTiO_3$ composites.[9,22]

Negative loss tangents observed in the vicinity of the transformation are indicative of material instability. These materials contain stored energy. The loss tangent is a measure of energy dissipation. A negative loss tangent indicates release of energy. The source of this energy is the partially constrained inclusions in the vicinity of an incipient phase transformation.

Thus far, anomalies in composites with phase-transforming inclusions have been observed during temperature sweeps. Stability limits for materials of this type under conditions of static or time-varying temperature are still under investigation.[24]

## Conclusions

Composites were successfully made with a zinc–aluminum (ZnAl) alloy matrix and silicon carbide particles. These composites exhibited a favorable combination of stiffness and viscoelastic damping. Composites of ZnAl–SiC were stiffer than the alloy matrix and exhibited higher damping at acoustic frequencies than the alloy matrix. Enhanced damping especially at higher frequencies, is attributed to misfit dislocations generated from differential thermal expansion between matrix and inclusion during solidification and cooling from the melt. ZnAl–SiC composites exhibited a higher figure of merit $E \tan \delta$ in comparison with the matrix; also a higher figure of merit than polymer damping layers and nanocomposites. ZnAl–$BaTiO_3$ composites exhibited anomalies in modulus and damping associated with partial restraint of phase transformation. One specimen had a Young's modulus much greater than that of diamond.

### Acknowledgment

Support by DARPA and NSF is gratefully acknowledged.

### References

1. Lakes RS. *Viscoelastic materials*. Cambridge: Cambridge University Press, 2009.
2. Capps RN and Beumel LL. Dynamic mechanical testing, application of polymer development to constrained layer damping. In: Corsaro RD and Sperling LH (eds) *Sound and vibration damping with polymers*. Washington DC: American Chemical Society, 1990.
3. Brodt M and Lakes RS. Composite materials which exhibit high stiffness and high viscoelastic damping. *J Compos Mater* 1995; 29: 1823–1833.
4. Ludwigson M, Swan CC and Lakes RS. Damping and stiffness of particulate SiC-InSn composite. *J Compos Mater* 2002; 36: 2245–2254.
5. Kim HJ, Swan CC and Lakes RS. Computational studies on high stiffness, high damping SiC-InSn particulate reinforced composites. *Int J Solids Struct* 2002; 39: 5799–5812.
6. Ritchie IG, Pan ZL and Goodwin FE. Characterization of the damping properties of die cast zinc aluminum alloys. *Metall Trans* 1991; 22A: 617–621.
7. Rundmann KB and Hilliard JE. Early stages of spinodal decomposition in an aluminum-zinc alloy. *Acta Metall* 1967; 15: 1025–1033.
8. Buhl H. *Advanced aerospace materials*. New York, NY: Springer, 1992.
9. Jaglinski T, Stone DS, Kochmann D and Lakes RS. Materials with viscoelastic stiffness greater than diamond. *Science* 2007; 315: 620–622.
10. Li X, Yang Y and Weiss D. Theoretical and experimental study on ultrasonic dispersion of nanoparticles for strengthening cast Aluminum Alloy A356. *Metall Sci Technol* 2008; 26(2): 12–20.
11. Brodt M, Cook LS and Lakes RS. Apparatus for measuring viscoelastic properties over ten decades: refinements. *Rev Sci Instrum* 1995; 66(11): 5292–5297.
12. Chen CP and Lakes RS. Apparatus for determining the viscoelastic properties of materials over ten decades of frequency and time. *J Rheol* 1989; 33: 1231–1249.
13. Demarest HH Jr. Cube-resonance method to determine the elastic constants of solids. *J Acoust Soc Am* 1971; 49: 768–775.
14. Wang YC, Ludwigson M and Lakes RS. Deformation of extreme viscoelastic metals and composites. *Mater Sci Eng A* 2004; 370: 41–49.
15. Hashin Z and Shtrikman S. A variational approach to the theory of the elastic behavior of multiphase materials. *J Mech Phys Solids* 1963; 11: 127–140.
16. Lakes RS, Kose S and Bahia H. Analysis of high volume fraction irregular particulate damping composites. *ASME J Eng Mater Technol* 2002; 124: 174–178.
17. Lucignano C, Quadrini F and Santo L. Dynamic mechanical performances of polyester-clay nanocomposite thick films. *J Compos Mater* 2008; 42: 2841–2852.
18. Suhr J, Koratkar N, Keblinski P and Ajayan P. Viscoelasticity in carbon nanotube composites. *Nat Mater* 2005; 4: 134–137.
19. Suhr J, Zhang W, Ajayan PM and Korathar NA. Temperature activated interfacial friction damping in carbon nanotube polymer composites. *Nano Lett* 2006; 6: 219–223.
20. Jaglinski T and Lakes RS. Anelastic instability in composites with negative stiffness inclusions. *Philos Mag Lett* 2004; 84: 803–810.
21. Ko JH, Kojima S, Koo TY, Jung JH, Won CJ and Hur NJ. Elastic softening and central peaks in $BaTiO_3$ single crystals above the cubic-tetragonal phase transition temperature. *Appl Phys Lett* 2008; 93: 102–905.
22. Castillo M. Project report. *Phase transforming composites*, University of Wisconsin-Madison 2006.
23. Dong L, Stone DS and Lakes RS. An elastic anomalies and negative Poisson's ratio in tetragonal $BaTiO_3$ ceramics. *Appl Phys Lett* 2010; 96: 141–904.
24. Kochmann DM and Drugan WJ. Dynamic stability of an elastic composite material having a negative-stiffness phase. *J Mech Phys Solids* 2009; 57: 1122–1138.